

DESIGN OF PHOTONIC CRYSTAL SLAB STRUCTURES WITH ABSOLUTE GAPS IN GUIDED MODES

C. G. Bostan, R. M. de Ridder

Lightwave Devices Group, MESA⁺ Research Institute, University of Twente,
P.O.Box 217, 7500 AE Enschede, The Netherlands

Both symmetric and asymmetric photonic crystal slabs with non-circular holes have been investigated. An absolute band gap was found for a triangular lattice of hexagonal holes in both symmetric and asymmetric slabs, but a square lattice of square holes has an absolute bandgap only in symmetric slabs. The band gap could be maximized by optimizing the angular orientation of the holes with respect to the lattice, leading to a larger gap than can be obtained with circular holes. The slab thickness was found to be an important tuning parameter for obtaining an absolute bandgap, and the sensitivity of the gap size to this parameter is shown.

(Received September 20, 2002; accepted October 31, 2002)

Keywords: Photonic crystal, Absolute band gap

1. Introduction

Photonic crystals (PhCs) have been the subject of intensive research for the last 15 years.

These are artificially made materials with spatially periodic distribution of dielectric permittivity. What makes PhCs special is their 'photonic bandgap' (PBG) property – a frequency range in which the electromagnetic waves' propagation is forbidden, regardless the wavevector and polarization state. Stated differently, a PhC is an omnidirectional optical isolator for frequencies inside the PBG, but only if the periodicity is 3D.

Defects can be introduced in PhCs by locally breaking the translational symmetry. They create states inside the PBG that are spatially localized in the defect regions. This fact has important applications for integrated-optical devices, in reducing their size and increasing the packaging density. A point defect can be a wavelength-scale resonant cavity with small modal volume and high quality factor [1]. A line defect can represent a waveguide that transfers light around sharp corners with high efficiency [2].

Anyway, the defects need to be shielded from the outside world to prevent radiation losses. Perfect shielding requires PhCs with full 3D PBGs.

However, it is still very difficult to integrate 3D PhCs with the existing planar technology. Instead, the goal of 3D control of light propagation can be accomplished by using quasi-2D PhCs, known also as 'photonic crystal slabs (PCS)'. A typical PCS structure consists in a high-refractive index plate (e.g. Si, GaAs) perforated with a 2D periodic lattice of air holes and having a thickness around half-wavelength. The plate is sandwiched between two semi-infinite regions that can be either homogeneous or patterned. There are two coexisting confinement mechanisms in a PCS: in-plane confinement-given by the PBG effect- and vertical confinement-given by refractive index contrast between the PCS and its claddings.

Because of its finite thickness, a PCS supports guided modes. If the slab has mirror-symmetry with respect to its horizontal middle plane, a gap between guided modes of certain symmetry can be opened [3]. For example, a PCS with triangular lattice of circular holes has a large gap in even modes. There are several reasons for which an absolute gap, independent of mode symmetry, would be a desirable feature. First, coupling between modes of opposite symmetry is possible in real structures;

because of fabrication intrinsic imperfections, the boundaries are neither smooth nor straight; roughness-induced scattering at the boundaries is important in a PCS where the number of boundaries is large. Second, a reasonable coupling efficiency between PCS and a ridge waveguide would need careful control over the polarization state. Third, the condition of mirror symmetry leads to an increase in the complexity of the fabrication process in certain cases (for example, when using silicon-on-insulator –SOI wafers).

To the best of our knowledge, a PCS with a significant absolute gap in guided modes was discussed only recently [4]. The example considered in this reference is the familiar triangular lattice of air holes in a PCS with mirror symmetry. In this paper we present and compare two new structures based on silicon-on-insulator (SOI) substrates, having large, absolute gaps in guided modes. We present a design procedure and computations of dispersion diagrams. Fully-vectorial eigenmodes of Maxwell's equations with periodic boundary conditions were computed by preconditioned conjugate-gradient minimization of the block Rayleigh quotient in a planewave basis, using a freely available software package [5]. Limits imposed by the lithography accuracy are considered.

The paper is organized as follows. In section 2 we discuss the band diagrams of selected 2D PhCs with large, absolute PBGs. These 2D PhCs are translated into their PCS-type brethren in section 3 and dispersion curves of guided modes are calculated. In section 4 conclusions are drawn and further possible developments are highlighted.

2. Two-dimensional PhCs

A PCS is obtained from its 2D PhC counterpart by truncating the infinite thickness down to a fraction of the lattice constant. The modes of the PCS-structure have a lower effective index, resulting in a shift of its band diagrams towards higher frequencies. Then, if the initial 2D PhC has an absolute (that is polarization-independent) PBG, this may be preserved in the PCS, depending on its thickness. On the other hand, one can infer that a 2D PhC that does not have a PBG in either TE or TM polarizations can be discarded for practical purposes, since the resulting PCS will not have a gap in guided modes.

Therefore, calculations of 2D PhCs provide a good starting point in selecting promising structures for PCSs. Moreover, the calculation time is orders of magnitude shorter than that for 3D structures.

Optimization of the PBG is very difficult, because it involves solving a multiparametric inverse problem. There are countless combinations of lattice symmetry, scattering object shape, filling factor and refractive index contrast, but it is impossible to say which one gives the largest absolute PBG. A systematic algorithm is still lacking, and the design is based on several *rules of thumb*. It is known that absolute PBGs are favored in PhCs that satisfy the following criteria:

- Refractive index contrast is as high as possible;
- Brillouin zone is close to a circle;
- Shape of scattering objects matches the symmetry of Brillouin zone [6];
- The PhC is comprised of isolated dielectric islands connected by narrow veins (this implies a high filling-factor for the low-index material)

Wang et al [6] recently performed a study on band diagrams of a broad range of 2D PhCs. They showed that an effective way of overlapping the TE and TM bands is by rotating noncircular 2D rods around their vertical (infinite) axis. The non-circular scattering objects introduce an additional degree of freedom (i.e. rotation angle); this leads to an increased flexibility in the design, but also makes the optimization even harder.

Calculations of band diagrams are presented in many papers [7-10]. Sometimes, the authors considered 'exotic' materials (e.g tellurium [10]) or extreme filling factors.

Both approaches pose serious challenges to the technology for PCS.

In the design of a fabrication process for PCSs one usually starts from the available technology and high refractive index materials. Lithographic accuracy puts a lower boundary on the achievable thickness of the veins and this should be accounted for when performing calculations.

Our 2D calculations are targeted to PCS design using SOI, having a PBG centered at the telecom wavelength $\lambda = 1.55 \mu\text{m}$. Therefore, we consider only PhCs consisting of air holes etched vertically in a silicon slab ($n_{\text{Si}} = 3.45$).

In this section we discuss the band diagrams of selected 2D geometries that are shown to have large absolute PBGs:

- i) triangular lattice of hexagonal holes
- ii) square lattice of square holes;

We will refer to these briefly as ‘hexagon-type’ and ‘square-type’, respectively.

The band diagrams were studied as a function of two geometrical parameters: size of air rods and their angular orientation with respect to the lattice. The air holes filling factor should be high enough, consequently the size of holes varies over a limited range. In our design procedure we fix the size and vary the rotation angle, aiming at maximizing the PBG. Optimum results were obtained for the hexagon’s side $R = 0.5a$ and the square’s side $d = 0.8a$, respectively, where a is the lattice constant. These values will be assumed from now on in this paper.

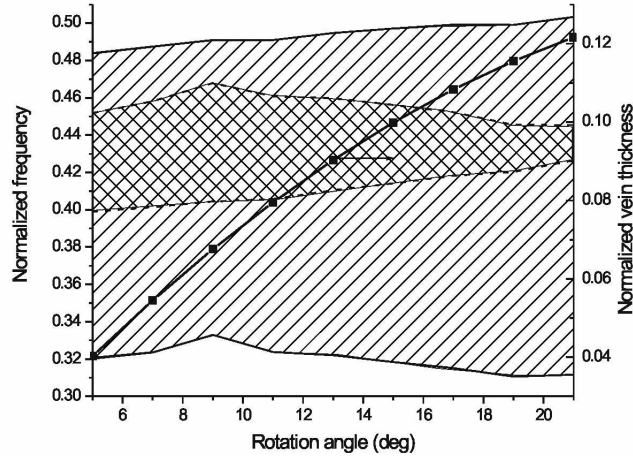


Fig. 1. Gap overlap as a function of rotation angle for a hexagon-type 2D PhC of air holes in a silicon background, hexagon side $R = 0.5a$; (right hatched: gap for TE polarization; cross-hatched: absolute band gap-coincides with gap for TM). The solid line shows the normalized vein thickness x_{hex}/a versus rotation angle.

In Fig. 1 we present the gaps for TE and TM polarizations and their overlap, as well as the veins’ thickness, as function of rotation angle, in hexagon-type geometry. The veins’ thickness in the triangular lattice is given by an analytical formula:

$$x_{\text{hex}} = a \sin(60^\circ + \alpha) - 2R \sin 60^\circ \quad (1)$$

For $\alpha = 0^\circ$ the corners of nearest-neighbor hexagons touch one another. The gap for TE is very large, completely enclosing the TM gap, so that the PBG coincides with the gap for TM. It is apparent that the maximum PBG is reached for $\alpha = 9^\circ$. The band diagrams for this rotation angle are shown in Fig. 2. The PBG is between $(0.4045 \dots 0.4679)(a/\lambda)$, with the center frequency $0.4362(a/\lambda)$ and normalized width of 14.5%.

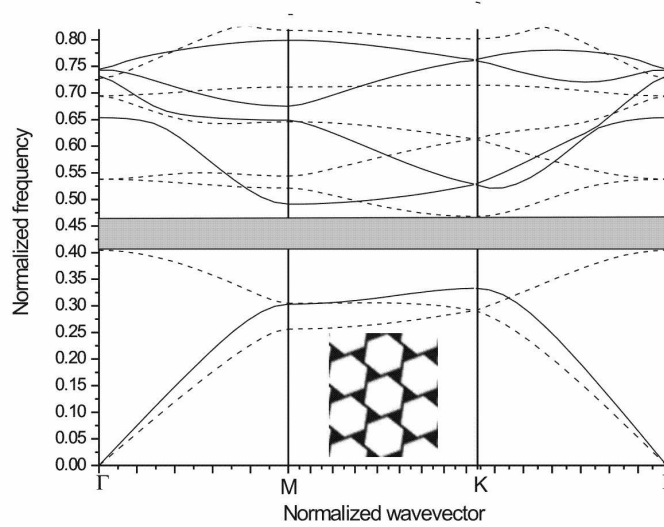


Fig. 2. Band diagrams for hexagon-type 2D PhC (shown in inset), with hexagon side $R = 0.5a$ and rotation angle $\alpha = 9^\circ$; solid and dash lines are bands for TE and TM polarizations, respectively; the PBG is shaded grey (width 14.5%).

In Fig. 3 we present the gaps for TE and TM polarizations and their overlap, as well as the veins' thickness, as function of rotation angle, in square-type geometry. The thickness of veins in the square lattice is:

$$x_{sq} = a \cos \alpha - d \tag{2}$$

The absolute PBG opens up for $\alpha = 24.5^\circ$ and its size increases monotonically as a function of rotation angle until $\alpha = 32^\circ$. The gap width dependence on α for square-type is more pronounced than that for hexagon-type. Band diagrams for $\alpha = 30^\circ$ are shown in Fig. 4. An absolute gap exist between $(0.4030 \dots 0.4463)(a/\lambda)$, with the center frequency $0.4246(a/\lambda)$ and normalized width of 10.2%.

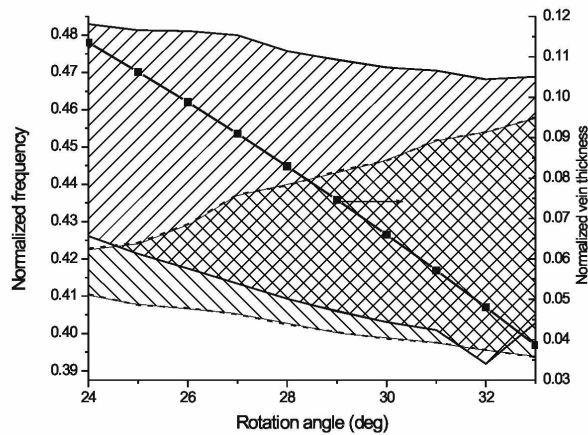


Fig. 3. Gap overlap as a function of rotation angle for a square-type 2D PhC of air rods in a silicon background, square side $d = 0.8a$; (right and left hatched are gaps for TE and TM polarizations, respectively; cross - hatched: absolute band gap). The solid line shows the normalized vein thickness x_{sq}/a versus rotation angle.

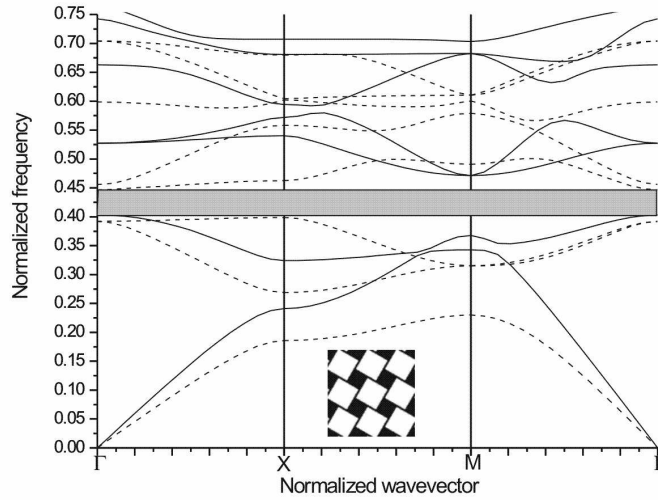


Fig. 4. Band diagrams for square-type 2D PhC (shown in inset), with square side $d = 0.8a$ and rotation angle $\alpha = 30^\circ$; solid and dash lines are bands for TE and TM polarizations, respectively; The PBG is shaded grey (width 10.2%).

3. Band diagrams of photonic crystal slabs

Up to now, the most studied PCS geometry has been the mirror-symmetric slab with a triangular lattice of circular air holes. This configuration is known to have a large gap in guided even modes and a smaller gap for odd guided modes. Under certain circumstances [4], these gaps can be made to overlap, leading to an absolute gap of about 8.5%.

In this section we show that large absolute gaps are achievable in both hexagon-type and square-type mirror-symmetric PCSs. Moreover, an absolute gap of more than 4% can be obtained in an asymmetric hexagon-type PCS.

The computational method requires a periodic cell. The PCS is patterned with a 2D periodic lattice and, in order to ensure 3D periodicity, we take a sequence of slabs periodical in the vertical direction (supercell) [3]. The period of the latter should be large enough so that the coupling among guided modes in adjacent slabs is negligible.

The light cone divides the ω - k plane into two regions. Modes situated below the light-cone are confined in the slab and decay exponentially in the claddings. Modes above the light-cone are leaking into the claddings and they are interacting with one another. Consequently the modes' frequencies calculated by the supercell method are false and we omit them from the graphical representation.

During the numerical experiments we observed that, when slab thickness (h) is varied, the frequencies of odd modes are shifting at a higher rate than the frequencies of the even modes. Thus, h can be used for optimizing the absolute gap size.

We proceed now to calculating dispersion curves in PCSs, using the optimum geometry parameters (R or d ; α) for air holes in silicon, as obtained in sec. 2. These optima might shift when moving from the purely 2D case to the slab geometry, possibly allowing further optimization, which has not been pursued in this work.

Depicted in Fig. 5 are band diagrams of guided modes in a hexagon-type symmetric PCS with air claddings and optimum thickness $h = 0.59a$. The absolute PBG is bounded by the second and third odd modes and the light cone and has 10.2% width. The tolerance of gap width with respect to h is addressed in Fig. 6: for $h = (0.575 \cdots 0.608)a$, the gap width is larger than 8%. Considering the midgap frequency for $\lambda = 1.55 \mu\text{m}$, we get $a = 777 \text{ nm}$, $R = 388 \text{ nm}$, $h = 458 \text{ nm}$, $x_{\text{hex}} = 52 \text{ nm}$.

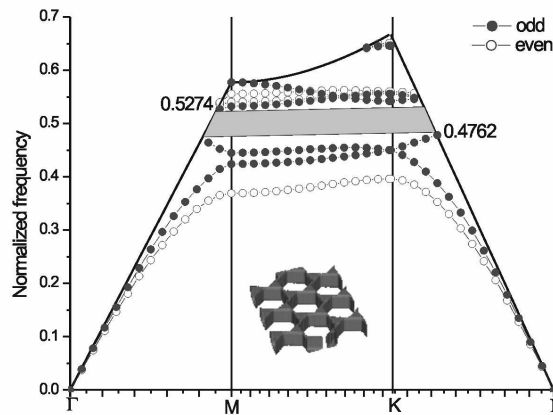


Fig. 5. Band diagrams of guided modes in a symmetric hexagon-type PCS with air claddings (shown in inset); parameters: $R = 0.5a$, $\alpha = 9^\circ$, $h = 0.59a$; (central frequency of the absolute gap: $f_0 = 0.5018a$, gap width: 10.2%).

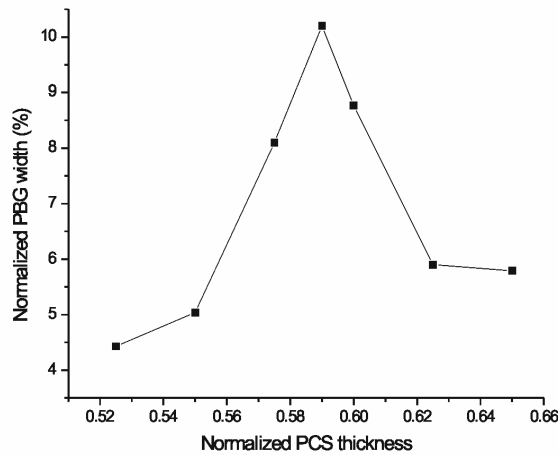


Fig. 6. Gap width vs slab thickness in a hexagon-type PCS with air claddings; parameters: $R = 0.5a$, $\alpha = 9^\circ$.

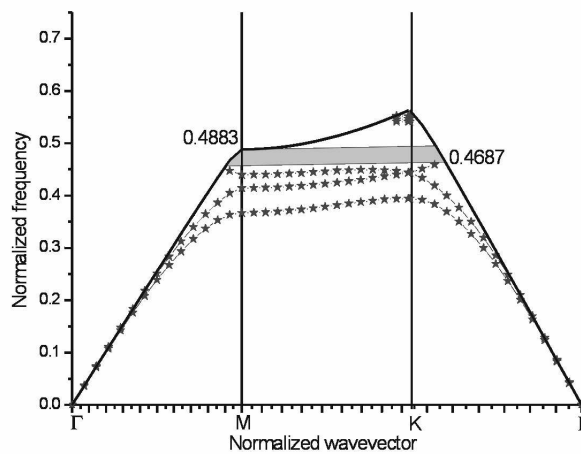


Fig. 7. Band diagrams of guided modes in an asymmetric hexagon-type PCS with an air upper-cladding and a silicon dioxide bottom-cladding both with thickness $4a$; the other parameters are the same as in Fig. 5; the air holes are penetrating the bottom-cladding; the light cone is determined by the first TM band of the bottom-cladding regarded as 2D PhC; (central frequency of the absolute gap: $f_0 = 0.4785a$, gap width: 4.1%).

When the hexagon-type PCS is asymmetric, with air and deeply etched silicon-dioxide ($n_{SiO_2} = 1.45$) upper and bottom claddings, respectively, the holes need to be etched through, deeply into the SiO_2 in order to maximize the bandgap. The resulting PBG for this case is reduced to 4.1%, as shown in Fig. 7. This happens because the light cone is shifted towards lower frequencies, which are determined by the first TM band of the 2D PhC bottom cladding.

Results for symmetric and asymmetric square-type PCS are shown in Fig. 8 and Fig. 9, respectively.

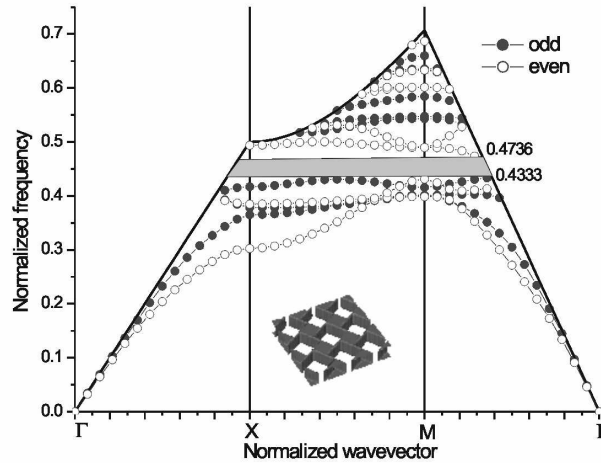


Fig. 8. Band diagrams of guided modes in a symmetric square-type PCS with air claddings (shown in inset); parameters: $d = 0.8a$, $\alpha = 30^\circ$, $h = 0.6a$; (central frequency of the absolute gap: $f_0 = 0.4534a$, gap width: 8.88%).

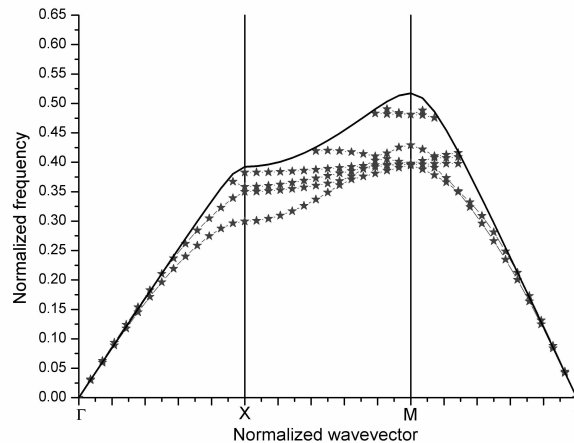


Fig. 9. Band diagrams of guided modes in an asymmetric square-type PCS with an air upper-cladding and a silicon dioxide bottom-cladding both with thickness $4a$; the other parameters are the same as in Fig. 8; the air holes are penetrating the bottom-cladding; the light cone is determined by the first TM band of the bottom-cladding regarded as 2D PhC; there is no bandgap present.

While the symmetric PCS with air claddings has a PBG of 8.88% width for the optimum thickness $h = 0.6a$, the asymmetric one does not show any PBG. This time, an extremely small departure from the optimum thickness makes the gap disappear; so, the fabrication of a square-type PCS would be a very critical process.

When the midgap frequency is chosen $\lambda = 1.55 \mu\text{m}$, it follows $a = 703 \text{ nm}$, $d = 562 \text{ nm}$, $h = 422 \text{ nm}$, $x_{sq} = 46 \text{ nm}$.

4. Discussion

We have presented the design of two PCS structures, labeled as ‘hexagon-type’ and ‘square-type’ respectively. Both can have large, polarization independent gaps in guided modes, in case of vertical mirror-symmetry and air claddings.

It turned out that ‘hexagon-type’ PCS has better performance than the ‘square-type’: a) its absolute gap is less sensitive to variations of geometrical parameters; b) the gap in even modes is very large (then, the probability of obtaining an overlap with the gap for odd modes is higher); c) the absolute gap is still present even in asymmetric PCSs.

When the PBG is absolute the mirror symmetry is no longer a crucial factor; this opens the possibility of reducing complexity of the technological process when using common SOI wafers leading to devices that are both mechanically and thermally more stable.

The design presented here is the basis of a fabrication process that is currently under way. The experimental results will be presented in a following paper.

Photonic crystal slabs with polarization independent gaps will form a platform for integration of ‘defect-based’ components (e.g. line defects, bends).

References

- [1] P. R. Villeneuve, S. Fan, J. D. Joannopoulos, "Microcavities in photonic crystals: Mode symmetry, tunability, and coupling efficiency," *Phys. Rev. B* **54**(11), 7837-7842 (1996).
- [2] A. Mekis, J. C. Chen, I. Kurland, S. Fan, P. R. Villeneuve, J. D. Joannopoulos, "High transmission through sharp bends in photonic crystal waveguides," *Phys. Rev. Lett.* **77**(18), 3787-3790 (1996).
- [3] S. G. Johnson, S. Fan, P. R. Villeneuve, J. D. Joannopoulos, L. A. Kolodziejcki, "Guided modes in photonic crystal slabs," *Phys. Rev. B* **60**(8), 5751-5758 (1999).
- [4] C. Jamois, R. B. Wehrspohn, J. Schilling, F. Muller, R. Hillebrand, W. Hergert, "Silicon-based photonic crystal slabs: two concepts," *IEEE J. Quantum Electron.* **38**(7), 805-810 (2002).
- [5] S. G. Johnson, J. D. Joannopoulos, "Block-iterative frequency-domain methods for Maxwell's equations in a planewave basis," *Opt. Express* **8**(3), 173-190 (2001).
- [6] R. Wang, X.-H. Wang, B.-Y. Gu, G.-Z. Yang, "Effects of shapes and orientations of scatterers and lattice symmetries on the photonic band gap in two-dimensional photonic crystals," *J. Appl. Phys.* **90**(9), 4307-4313 (2001).
- [7] M. Plihal, A. A. Maradudin, "Photonic band structures of two-dimensional systems: The triangular lattice," *Phys. Rev. B* **44**(16), 8565-8571 (1991).
- [8] R. Padjen, J. M. Gerard, J. Y. Marzin, "Analysis of the filling pattern dependence of the photonic bandgap for two-dimensional systems," *J. Mod. Opt.* **41**(2), 295-310 (1994).
- [9] Y. Chen, "Photonic band gaps of two-dimensional photonic lattices: the face-centered graphite structures," *Superlattices and Microstructures* **22**(1), 115-199 (1997).
- [10] Z.-Y. Li, Y. Xia, "Omnidirectional absolute band gaps in two-dimensional photonic crystals," *Phys. Rev. B* **64**(15), 153108 (2001).